Mechanisms of Allosteric Regulation of *Trypanosoma cruzi S*-Adenosylmethionine Decarboxylase[†]

Tracy Clyne Beswick, Erin K. Willert, and Margaret A. Phillips*

Department of Pharmacology, University of Texas Southwestern Medical Center at Dallas, 6001 Forest Park Boulevard, Dallas, Texas 75390-9041

Received February 27, 2006; Revised Manuscript Received May 2, 2006

ABSTRACT: *S*-Adenosylmethionine decarboxylase (AdoMetDC) is a pyruvoyl-dependent enzyme that catalyzes an essential step in polyamine biosynthesis. The polyamines are required for cell growth, and the biosynthetic enzymes are targets for antiproliferative drugs. The function of AdoMetDC is regulated by the polyamine-precursor putrescine in a species-specific manner. AdoMetDC from the protozoal parasite *Trypanosoma cruzi* requires putrescine for maximal enzyme activity, but not for processing to generate the pyruvoyl cofactor. The putrescine-binding site is distant from the active site, suggesting a mechanism of allosteric regulation. To probe the structural basis by which putrescine stimulates *T. cruzi* AdoMetDC we generated mutations in both the putrescine-binding site and the enzyme active site. The catalytic efficiency of the mutant enzymes, and the binding of the diamidine inhibitors, CGP 48664A and CGP 40215, were analyzed. Putrescine stimulates the k_{cat}/K_m for wild-type *T. cruzi* AdoMetDC by 27-fold, and it stimulates the binding of both inhibitors (IC_{50}s decrease 10−20-fold with putrescine). Unexpectedly CGP 48664A activated the *T. cruzi* enzyme at low concentrations (0.1−10 μM), while at higher concentrations (>100 μM), or in the presence of putrescine, inhibition was observed. Analysis of the mutant data suggests that this inhibitor binds both the putrescine-binding site and the active site, providing evidence that the putrescine-binding site of the *T. cruzi* enzyme has broad ligand specificity. Mutagenesis of the active site identified residues that are important for putrescine stimulation of activity (F7 and T245), while none of the active site mutations altered the apparent putrescine-binding constant. Mutations of residues in the putrescine-binding site that resulted in reduced (S111R) and enhanced (F285H) catalytic efficiency were both identified. These data provide evidence for coupling between residues in the putrescine-binding site and the active site, consistent with a mechanism of allosteric regulation.

S-Adenosylmethionine decarboxylase (AdoMetDC[1]) catalyzes a key step in the biosynthesis of the polyamines spermidine and spermine (*1*, *2*). Polyamines are essential for cell growth, and inhibitors of polyamine biosynthesis have demonstrated antiproliferative effects (*3*). The most effective clinical application of these inhibitors is for the treatment of African sleeping sickness caused by the parasitic protozoa, *Trypanosoma brucei*. α-Difluoromethylornithine, a suicide inhibitor of ornithine decarboxylase (ODC), is used clinically to treat this disease (*4*). Additionally, inhibitors of AdoMetDC have efficacy in animal models of both *T. brucei* (*5*−*7*) and a related parasite *Trypanosoma cruzi* (*8*), which is the causative agent of Chagas disease. In contrast to *T. brucei*, *T. cruzi* does not contain ODC and instead salvages putrescine from the host (*9*). *T. cruzi* however maintains a functional AdoMetDC, and the finding that inhibitors of AdoMetDC reduce infectivity by the parasites suggests that the function of this enzyme is not fully replaced by the ability of the parasite to transport polyamines from the host cell. It is also noteworthy that the trypanosomatidae synthesize a unique polyamine that is a conjugate of spermidine and gluthathione, termed trypanothione (*10*). A number of potent inhibitors of human AdoMetDC have been described, including reversible substrate analogues and mechanism based inhibitors (*1*) (Chart 1). However, MGBG (methylglyoxal bis(guanylhydrazone)) is a much less potent inhibitor of the *T. cruzi* enzyme (*11*), suggesting that inhibitors of the human enzyme are unlikely to be optimized for binding to the parasite AdoMetDC.

AdoMetDC belongs to the family of decarboxylases that utilize a pyruvoyl cofactor to facilitate catalysis. The pyruvoyl cofactor is generated in an autocatalytic reaction that results in the cleavage of the peptide backbone and formation of pyruvate from a serine residue (position 68 in the human enzyme). A series of crystallographic (*12*−*15*) and mutagenic (*16*−*20*) studies on human AdoMetDC have elucidated both the mechanism of proenzyme processing and the nature of the enzyme active site (Figure 1). Single-turnover analysis of the *T. cruzi* enzyme demonstrated that the rate-limiting step in the reaction occurs after decarboxylation, and is likely to be Schiff base hydrolysis/product release (*21*).

[†] This work was supported by National Institutes of Health grants (R01 AI34432) (to M.A.P.) and predoctoral fellowship (GM007062) (to E.K.W.) and the Welch Foundation Grant I-1257 (to M.A.P.).

* Author to whom all correspondence should be addressed. Tel: (214) 645-6164. Fax: (214) 645-6166. E-mail: margaret.phillips@UTSouthwestern.edu.

[1] Abbreviations: AdoMetDC, *S*-adenosymethionine decarboxylase; MGBG, methylglyoxal bis(guanylhydrazone); CGP 48664A, 4-amidinoindan-1-one-2′-amidinohydrazone; CGP 40215, 1,3-bis[(3′-amidinobenzylidene)amino]guanidine.

10.1021/bi0603975 CCC: $33.50
Published on Web 06/03/2006

Chart 1: Structures of AdoMetDC Active Site Inhibitors

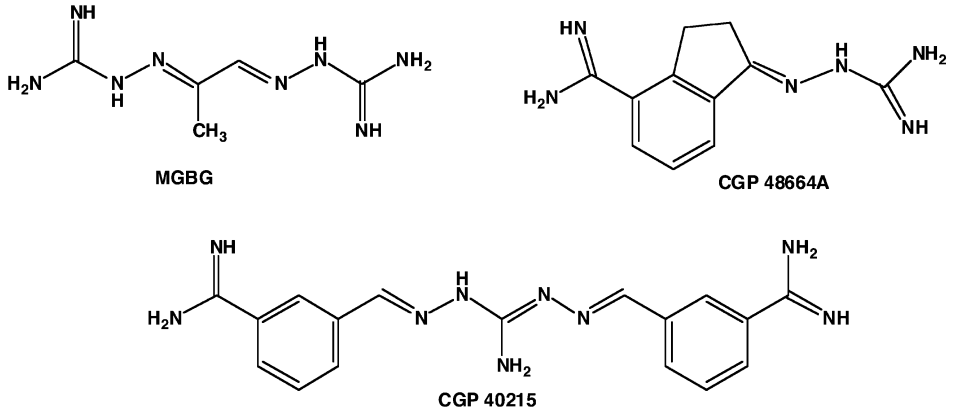

Putrescine, the product of the ODC reaction, and the precursor to spermidine, has been demonstrated to stimulate both the processing reaction and the catalytic efficiency of the enzyme. However, the effect of putrescine on these properties is highly species specific. Putrescine is reported to stimulate both the processing and the activity of the human enzyme (*13*, *16*, *17*, *19*, *20*), while the enzyme from plants is not affected by putrescine (*15*, *22*−*24*). The enzyme activity of the *T. cruzi* enzyme is stimulated by putrescine; however, even under conditions of maximal activity, it is still a much less catalytically efficient enzyme than either the human or plant enzymes (*11*, *21*, *25*, *26*). Putrescine has been shown to stimulate the enzyme activity of a number of other eukaryotic enzymes, including the enzymes from *T. brucei*, yeast, and worm (*27*−*31*). Less is known about the effects of processing on these other enzymes; however, the processing reaction of the *T. cruzi* enzyme has been studied in detail, and it is not affected by putrescine (*26*).

The X-ray structure of human AdoMetDC demonstrates that putrescine is bound between the β-sandwich protein core, in a highly charged region that is 15 Å from the active site pyruvate, suggesting that an allosteric mechanism controls putrescine stimulation of activity and processing (*13*) (Figure 1). In comparison the X-ray structure of the potato enzyme reveals that amino acid substitutions in the putrescine-binding site, largely with positively charged residues, have occluded this site, and allowed the formation of a hydrogen bonding network at this site (*15*). These amino acid substitutions apparently allow the plant enzyme to be fully active in the absence of putrescine.

While an X-ray structure of the *T. cruzi* enzyme is not available, the available human and plant AdoMetDC structures provide models to study the structural basis for the effects of putrescine on the *T. cruzi* enzyme. Like the plant enzyme, *T. cruzi* AdoMetDC contains an Arg at position 13 (Figure 1). Mutation of this residue to the corresponding residue in the human structure (Leu13) abolishes processing of the *T. cruzi* enzyme; thus, a positively charged residue in this position appears to substitute for putrescine in the processing reaction (*26*). In contrast the *T. cruzi* enzyme contains other residues in the putrescine-binding site that are more similar to those found in the human enzyme (e.g. D174). D174 in particular has been demonstrated to be important for putrescine binding and stimulation of putrescine activity in both the parasite (*26*) and human enzymes (*17*, *32*).

In order to more fully elucidate the allosteric mechanism by which putrescine stimulates the activity of the *T. cruzi* AdoMetDC, we generated a series of mutations in both the enzyme active site and the putrescine-binding site. The effects of these mutations on the catalytic efficiency of the enzyme, and on the binding of active site inhibitors, were analyzed. CGP 48664A was identified as a novel activator of the *T. cruzi* enzyme that is able to bind both the putrescine-binding site and the active site, suggesting that the *T. cruzi* enzyme can be activated by a diverse set of amines. The studies identify several residues that are likely to be important for communication between the putrescine-binding site and the active site, and thus provide insight into the mechanism of allosteric regulation. Finally the identification of a mutant enzyme that has higher catalytic efficiency than the wild-type enzyme shows that *T. cruzi* AdoMetDC is not optimally evolved for high efficiency catalysis, but instead has evolved a low activity enzyme that is sensitive to regulation by putrescine. These properties of the enzyme provide a mechanism by which the trypanosome parasites can control polyamine levels.

EXPERIMENTAL PROCEDURES

Materials. *S*-Adenosyl[*carboxyl*-^{14}C]methionine (^{14}C-AdoMet; 62 mCi/mmol) was purchased from Amersham Pharmacia Biotech (Arlington Heights, IL). Unlabeled *S*-adenosylmethionine was purchased from Sigma. Ni^{2+} agarose was purchased from Qiagen Inc. (Chatsworth, CA). QuikChange site-directed mutagenesis kit was purchased from Stratagene (La Jolla, CA). CPG 40215 and CGP 48664A were generous gifts from Novartis. MGBG and all other reagents were purchased from Sigma.

Methods. Expression and Purification of AdoMetDC. Both human and *T. cruzi* AdoMetDC were expressed and purified as an N-terminal 6 His-tagged fusion from a T7 bacterial expression construct as previously described (*25*). *Escherichia coli* BL21/DE3 cells containing the construct were grown in LB, and the recombinant enzymes were purified using Ni^{2+}-agarose column chromatography and anion exchange chromatography. All purification buffers lacked putrescine. The purified protein was quantified using the extinction coefficient previously determined for the native enzyme (46.5 mM^{-1} cm^{-1} for *T. cruzi*, 39.8 mM^{-1} cm^{-1} for human). The mole fraction of putrecine bound to the purified human enzyme was estimated as follows. Protein was denatured by boiling (10 min) and precipitated with 9% TCA.

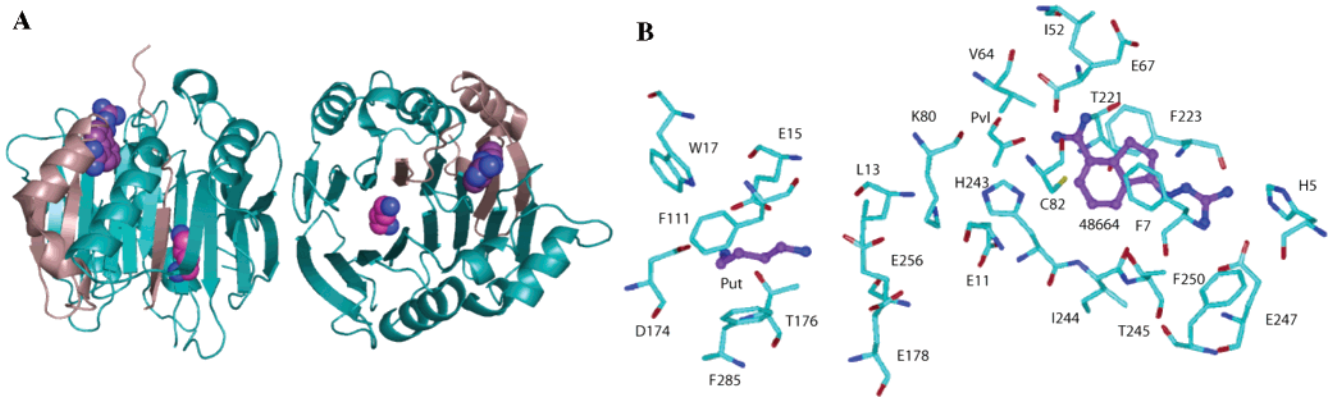

C

```
                                        5  7     13
human           ---------------------MEAAHFFEGTEKLLEVWFSRQQPDANQGSGDLRTIPRSE 39
potato          ----------------MEMDLPVSAIGFEGFEKRLEISFVEPGLFADPNGKGLRSLSKAQ 44
Tcruzi          MLSNKDPLSLMAMWGSVKGYDPNQGASFEGPEKRLEVIMR---IIDETHSEGLHALGDEV 57

                          52            64   68
human           WDILLKDVQCSIISVTKTDKQEAYVLSESSMFVSKRRFILKTCGTTLLLKALVPLLKLAR 99
potato          LDEILGPAECTIVDNLSNDYVDSYVLSESSLFVYSYKIIIKTCGTTKLLLAIPPILRLAE 104
Tcruzi          WKGVVGSLNAQIVSKESNEYIRSYVLTESSLFVMRDRIILITCGTTTLLNAVPFVLDAVS 117

                       111
human           DYSGFDSIQSFFYSRKNFMKPSHQGYPHRNFQEEIEFLNAIFPNGAG----YCMGRMN-S 154
potato          TLS--LKVQDVRYTRGSFIFPGAQSFPHRHFSEEVAVLDGYFGKLAAGSKAVIMGSPDKT 162
Tcruzi          DVRG--EVEWVSFMHKNYSFPWEQKGPHLSMAEEFNTLRTYFPSGKP----FIFGPVD-S 170

                                174
human           DCWYLYTLDFPESRVISQPDQTLEILMSELDPAVMDQFY----MKDGVTAKDVTRESGIR 210
potato          QKWHVYSASAG-SVQSNDPVYTLEMCMTGLDREKASVFY----KTEESSAAHMTVRSGIR 217
Tcruzi          DHYFLFVYDDVIRPCETENDTQLSMTMYGLDRTQTKHWFSDRFISTGTETAAIRKATKLD 230

                     221                     245 247 250
human           DLIPGSV-IDAIMFNPCGYSMNGMKSDGTYWTIHIIPEPEFSYVSFETN---LSQTSYDD 266
potato          KILPKSE-ICDFEFEPCGYSMNSIEG-AAVSTIHITPEDGFTYASFESVGYNPKTMELGP 275
Tcruzi          KVADDSWKLHDLQFEPCGYSINTIRG-AEYQTIHITPEDHCSFASYETN---TPAVNYSE 286

                           285
human           LIRKVVEVFKPGKFVTTLFVNQSSKCRTVLASP----QKIEGFKRLDCQSAMFNDYN--F 320
potato          LVERVLACFEPAAEFSVALHADVATKLLERICS-----VDVKGYSLAEWSPEEFGEGGS-I 329
Tcruzi          RINTVLGVFAPIRFSVIVFIDPDSDVGRLYQKGQNVGVEAEYYPKYELQNRTVNEFAPGY 346

human           VFTSFAKKQQQQQS----------------- 334
potato          VYQKFTRTPYCESPKSVLKGCWKEEEKEGKE 360
```

FIGURE 1: (A) Ribbon diagram of the human AdoMetDC dimer bound to putrescine (pink) and the active site inhibitor CGP 48664A (purple). The β-chain (N-terminus) is in pink, and the α-chain (C-terminus) is in turquoise (B) The structure of the putrescine and CGP 48664A binding sites in human AdoMetDC. Amino acid side chains are in turquoise. The pyruvoyl cofactor (Pvl) is the N-terminal residue of the α-chain. Figure 1A was created in PyMOL (Delano Scientific), and Figure 1B was created in Insight II (Accelrys) using the X-ray structure pdb file 1I7M (*14*, *15*) (C) Sequence alignment of the protein coding region for human, potato, and *T. cruzi* AdoMetDC. The residue numbers in the top line correspond to the numbering of the human sequence. Residues in the active site are colored in pink, and residues in the putrescine-binding site (as defined by the human enzyme structure) are in yellow.

Samples were clarified by centrifugation and labeled with AccQ·TAG reagent (Waters) according to the manufacturer's instructions. Derivatized samples (equivalent to 100 pmol protein mol/mol) were applied to an AccQ·TAG, and labeled amines in the sample were separated and detected as previously described (*33*).

Site-Directed Mutagenesis of T. cruzi AdoMetDC. To create mutant AdoMetDC enzymes, PCR-based site-directed mutagenesis using the Stratagene QuikChange kit was performed using the *T. cruzi* AdoMetDC expression plasmid as a template. The constructs were verified by sequencing. The amino acid numbering referenced in the manuscript is based on the human sequence as shown in the alignment in Figure 1A. The coding strand primers for the mutagenesis were as follows: D174V, CCATGTGAGACGGAGAACGTTACACAGTTGAGTATG; S111R, GGGGAGGTGGAATGGGTCAAGTCAATGCATAAG; F285H, CGTTTTTCCGTGATTGTCCACATTGATCCTGACAGTGATG; F7A, CCAAATCAGGGGGCCAGTGCTGAGGGGCGG; A5H, CGACCCAAATCAGGGGCACAGTTTTGAGGGG; V52I, GGCTCGTTAAATGCCCAAATTATATCCAAAGAGAGTAATGAG; V64A, GAGTATATTCGCTCTTATGCGCTAACGGAAAGCTCATTG; L221T, GACTCATGGAGGTTGCATGATACGCAATTTGAGCCGTGTGGG; F223A, GACTCATGGAAGTTGCATGATTTGCAAGCTGAGCCGTGTGGG; T245A, CAGACGATGCACATAGCACCGGAAGATCACTGC; E247A, CAGACGATGCACATAACACCAGCAGATCACTGC; C250F, CACATAACACCAGAAGATCACTTCTCTTTTGCCTCG.

Steady-State Kinetic Analysis. Steady-state kinetic analysis of AdoMetDC was performed as previously described (*25*). Reactions were carried out in buffer [100 mM Hepes pH

Table 1: Kinetic Parameters for Wild-Type *T. cruzi* and Human AdoMetDC and for Putrescine Binding Site Mutants of *T. cruzi* AdoMetDC[a]

	k_{cat}/K_m (M^{-1} s^{-1})[1]		CGP40215 IC_{50} (μM)		putrescine
[putrescine]:	0	5 mM	0	5 mM	K_{act} (mM)[b]
		A. Wild-Type AdoMetDC			
T. cruzi	3.5 ± 1.3	100 ± 25 (29)	32 ± 6	3.2 ± 0.8 (10)	0.42 ± 0.50
human	$2.5 \pm 0.6 \times 10^4$	$4.4 \pm 0.8 \times 10^4$ (2)	0.010 ± 0.003	0.006 ± 0.003 (2)	nd
		B. Mutant *T. cruzi* AdoMetDC			
S111R	2.0 ± 0.04	6.4 ± 0.26 (3)	96 ± 24	104 ± 48 (1)	7.9 ± 2.6
D174V	6.6 ± 0.29	5 ± 3.0 (1)	13 ± 4	14 ± 5 (1)	>45
F285H	1.8 ± 0.1	650 ± 200 (360)	26 ± 11	1.2 ± 1.2 (22)	0.31 ± 0.060

[a] Values in parentheses are the fold activation by putrescine. [b] Errors are standard errors of the fit. IC_{50} values are the averages of IC_{50} values (CGP 40215) determined at 3 different substrate concentrations (10, 32, and 80 μM) based on the relationship that $K_I = IC_{50}$, for noncompetitive inhibition (see Experimental Procedures), and the errors are standard deviations of the mean. nd = not determined.

8.0, 50 mM NaCl, and 5 mM DTT] at various ^{14}C-AdoMet concentrations (10−160 μM). Reaction mixtures were incubated at 37 °C for 10, 20 and 40 min at various enzyme concentrations (0.5−8 μM for *T. cruzi* and 5−20 nM for human AdoMetDC) to ensure a linear rate with time. Data points were collected in triplicate. Data were fitted to the Michaelis−Menten equation to determine K_m and k_{cat}. For enzymes in which the K_m was higher than the maximum substrate concentration used in our assay, k_{cat}/K_m was determined from the slope by fitting the linear portion of the velocity vs substrate curve. Dose response curves for k_{cat}/K_m at various putrescine concentrations (0−10 mM) were generated and the data were fitted to a one site hyperbolic binding model to derive an apparent dissociation binding constant (K_d) for putrescine activation, which we define as K_{act} (effective concentration required for 50% activation).

Kinetic Analysis of Inhibitor Binding. CGP 40215 or CGP 48664A (0−10 mM) was added to reaction mixtures containing a range of ^{14}C-AdoMet concentrations and enzyme (1−4 μM for *T. cruzi* AdoMetDC or 5−20 nM for human AdoMetDC). The data were fitted to dose−response curves to determine IC_{50} values. The inhibition patterns were consistent with noncompetitive inhibition, thus $IC_{50} = K_i$. For L221T in the presence of putrescine, the IC_{50} depends on the enzyme concentration consistent with tight binding inhibition. The data were fitted to the Morrison equation to determine the K_i^{app} (*34*).

HPLC Purification of CGP 48664A. To demonstrate that CGP 48664A, and not a contaminating compound, was responsible for the unusual activation kinetics of *T. cruzi* AdoMetDC, we purified the compound by reversed-phase ion-pairing column chromatography as described (*35*), except that the sample buffer and column eluent contained 10 mM CH_3SO_3H instead of pentane-sulfonic acid. CGP4866A was dissolved in buffer A (50 mM NaH_2PO_4/10 mM CH_3SO_3H pH = 3.0), incubated for 1 h, and applied (100 nmol of a 1 mM stock) to a 250 × 4.6 mm Nucleosil 5 μ C_{18} 100 Å HPLC column (Varian) equilibrated with buffer A. Sample was eluted isocratically with 20% buffer B (50 mM NaH_2PO_4/10 mM CH_3SO_3H/40% acetonitrile, pH = 3.0), and the absorbance of each fraction was monitored at 305 nm. A single peak was eluted at $t_R = 13.9$ min. The peak fraction was collected and the mass verified by positive ion electrospray mass spectral analysis ($m + 1 = 231$). The peak fraction demonstrated the same kinetic behavior as the original compound.

RESULTS

Steady-State Kinetic Analysis of Wild-Type T. cruzi and Human AdoMetDC. We previously characterized the effects of putrescine on the steady-state kinetics of wild-type *T. cruzi* AdoMetDC, and demonstrated a 9-fold maximal activation on k_{cat} (*25*). These data were collected with a mixture of ^{14}C-radiolabeled AdoMet (Amersham) and unlabeled compound (Sigma). Using the current batch of unlabeled AdoMet (Sigma) we were unable to demonstrate putrescine activation of the enzyme. To determine if impurities in the commercial AdoMet stocks accounted for the lack of reproducibility in the putrescine activation curve, cold AdoMetDC was left out of the reaction. Under these conditions the *T. cruzi* AdoMetDC activity was again strongly activated by putrescine. These data suggest that the cold AdoMet purchased from Sigma is contaminated with a small molecule that interferes with putrescine stimulation, and this contamination varies from batch to batch. It is likely to be at least a partial antagonist that binds the putrescine-binding site, since full activation of the enzyme cannot be obtained under conditions that include cold AdoMet. Thus, in order to measure the uncompromised effects of putrescine on the system, all further experiments were done with synthetically pure ^{14}C-radiolabeled AdoMet (Amersham). This limited the substrate concentration range (<160 μM) that could be practically used for kinetic analysis. Thus for enzymes where the K_m was significantly above this value we determined only the k_{cat}/K_m ratio, since the individual constants could not be determined with accuracy.

Steady-state kinetic data were collected for both *T. cruzi* and human AdoMetDC in the presence and absence of saturating concentrations (5 mM) of putrescine (Figure 2). For wild-type *T. cruzi* AdoMetDC, k_{cat} and K_m were found to be 0.0009 ± 0.0002 s^{-1} and 260 ± 20 μM, while the fully activated enzyme in the presence of 5 mM putrescine has a k_{cat} and K_m of 0.024 ± 0.001 s^{-1} and K_m of 250 ± 80 μM, respectively. This represents a 27-fold activation of k_{cat} (Table 1), which is significantly higher than previously reported (*11*, *25*). The concentration of putrescine required for maximal activation was confirmed by determining the k_{cat}/K_m over a range of putrescine concentrations. The dependence of activity on putrescine concentration displayed saturation kinetics and when fitted to a one-site binding model yielded an apparent dissociation constant (concentration of half-maximal activation) of $K_{act} = 0.42$ mM, lower than previously reported ($K_{act} = 2.5$ mM (*25*)). This value, however, is in good agreement with the K_d (0.15−0.2 mM)

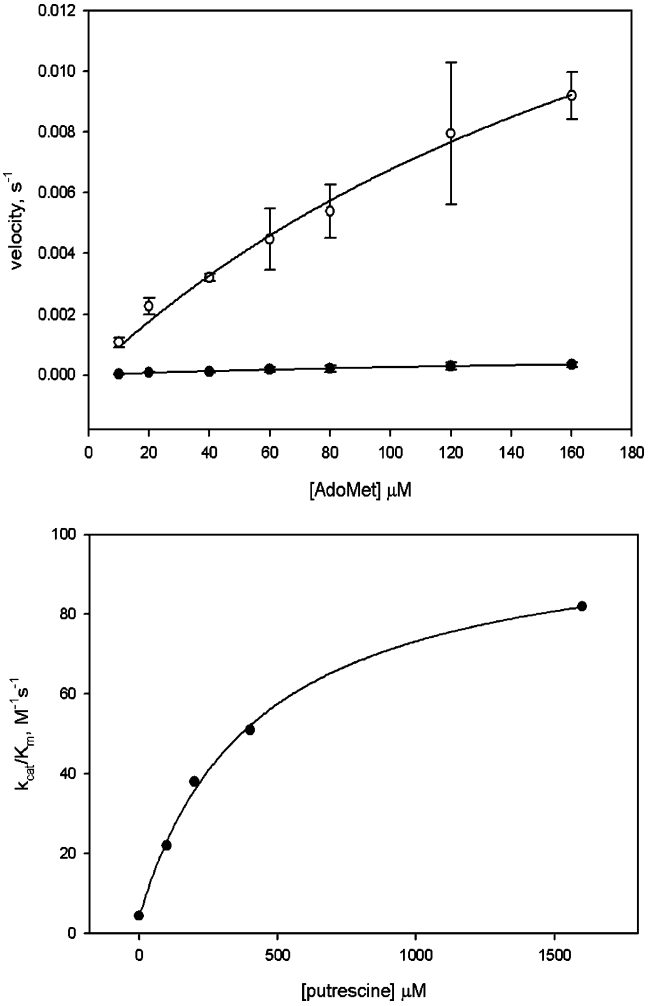

FIGURE 2: (A) Steady-state kinetic analysis of wild-type *T. cruzi* AdoMetDC (1 μM), in the presence (open circles) or absence (closed circles) of 5 mM putrescine. Error bars are standard error of the mean. The data were fitted to the Michaels−Menten equation to determine the kinetic parameters: No putrescine $K_m = 260 \pm 20$ μM, $k_{cat} = 0.0009 \pm 0.0002$ s^{-1}, and 5 mM putrescine $K_m = 250 \pm 80$ μM, $k_{cat} = 0.024 \pm 0.001$ s^{-1}. Errors are standard error of the fit. (B) Effects of putrescine on *T. cruzi* AdoMetDC. Values for k_{cat}/K_m were determined at different putrescine concentrations, and the concentration of putrescine required for half-maximal activation ($K_{act} = 420 \pm 50$ μM) was calculated from the fit of these data to a one-site hyperbolic binding model.

measured by fluorescence and radiolabeled-ligand binding assays (*26*).

The steady-state kinetic parameters for human AdoMetDC were also measured in the absence ($k_{cat} = 1.9$ s^{-1} and $K_m = 74$ μM) and presence of putrescine ($k_{cat} = 2.6$ s^{-1} and $K_m = 59$ μM), representing a 1.7-fold increase in catalytic efficiency (Table 1) somewhat lower than the 4−7-fold activation which has been previously reported (*20*, *32*). This minimal level of activation suggests that the human enzyme contains bound putrescine prior to the addition of the activator during kinetic analysis. To estimate the amount of putrescine bound to the purified enzymes, protein was denatured and polyamine content was determined by derivatization with a fluorescent label followed by HPLC (Experimental Procedures). The purified human enzyme was associated with 0.5 mol of putrescine/mol of protein, consistent with the observation that only 2-fold activation was achieved upon the addition of free putrescine. The

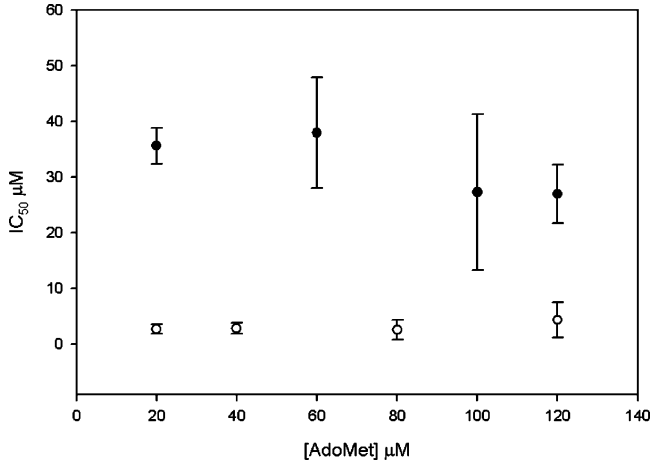

FIGURE 3: Inhibition of *T. cruzi* AdoMetDC by CGP 40215. Plot of IC_{50} versus the concentration of the substrate AdoMet. Data were collected in the absence (closed circles) or presence (open circles) of 5 mM putrescine. Errors are standard deviations of the mean ($n = 3$).

finding that putrescine remains bound to human AdoMetDC during purification, despite extensive washing of the protein during column chromatography, is consistent with previous observations that the human enzyme differs from the parasite enzyme and binds putrescine with high affinity (*12*, *21*).

The Effects of Putrescine on Inhibition of Wild-Type T. cruzi and Human AdoMetDC by CGP 40215 and CGP 48664A. While the effects of putrescine on the substrate turnover have been previously characterized for these enzymes, studies to determine if putrescine can also affect the binding of inhibitors have not been reported. CGP 40215 and CGP 48664A are analogues of MGBG (Chart 1). CGP 48664A has been cocrystallized with human AdoMetDC and demonstrated to bind in the active site (*14*). Inhibitor studies were undertaken for wild-type *T. cruzi* and human AdoMetDC. For *T. cruzi* AdoMetDC the IC_{50} for CGP 40215 is constant over a range of substrate concentrations indicative of noncompetitive inhibition (Figure 3, Table 1). The IC_{50} was calculated to be 32 μM in the absence of putrescine and 3 μM in the presence of 5 mM putrescine. For noncompetitive inhibition the $IC_{50} = K_i$, thus these data demonstrate that putrescine increases the binding affinity of the inhibitor to the *T. cruzi* enzyme. CGP 40215 binds human AdoMetDC with much higher affinity (3200-fold) than to the *T. cruzi* enzyme, and putrescine decreased the IC_{50} by 1.7-fold, similar to the effects on activity (Table 1). The observation of noncompetitive inhibition is not readily understood from the available data. Both substrate and inhibitor bind the active site (Figure 1B), suggesting either that the active site is large enough to accommodate both or that a more complex kinetic model is required to fully explain the data.

The situation is further complicated with respect to CGP 48664A. For the human enzyme, the IC_{50} values were again constant over a range of substrate concentrations indicating noncompetitive kinetics ($IC_{50} \pm 5$ mM putrescine is 3−5 nM). *T. cruzi* AdoMetDC, however, showed a distinct response to CGP 48664A inhibition. At lower drug concentrations (<10 μM), the compound activated the enzyme, but at concentrations above this level the enzyme is inhibited, and the apparent IC_{50} was in the range of 100 μM (Figure

Table 2: Kinetic Parameters for Active Site Mutants of *T. cruzi* AdoMetDC[a]

	k_{cat}/K_m (M^{-1} s^{-1})[1]		CGP40215 IC_{50} (μM)		
[putrescine]:	0	5 mM	0	5 mM	putrescine K_{act} (mM)[b]
wild-type	3.5 ± 1.3	100 ± 25 (29)	32 ± 6	3.2 ± 0.8 (10)	0.42 ± 0.50
A5H	2.2 ± 0.06	77 ± 9 (35)	13 ± 3	5 ± 5 (3)	0.21 ± 0.12
F7A	0.13 ± 0.01	0.55 ± 0.13 (4)	26 ± 6	7 ± 0 (4)	0.32 ± 0.06
V52I	3.7 ± 0.14	94 ± 41 (25)	18 ± 6	4 ± 4(5)	0.34 ± 0.27
V64A	0.40 ± 0.06	5 ± 1.5 (13)	150 ± 40	13 ± 10 (12)	0.79 ± 0.40
L221T	1.8 ± 0.19	32 ± 2.0 (18)	9.5 ± 4.5	0.4 ± 0.23[c] (24)	0.44 ± 0.04
T245A	0.77 ± 0.05	2.8 ± 0.3 (4)	440 ± 100	34 ± 13 (13)	0.53 ± 0.05
E247A	0.21 ± 0.021	3.6 ± 0.5 (17)	4100 ± 680	88 ± 78 (46)	0.33 ± 0.15
C250F	1.4 ± 0.05	14 ± 3 (10)	28 ± 8	4 ± 2 (7)	0.47 ± 0.1
D174V/E247A	0.48 ± 0.01	0.47 ± 0.02 (1)	124 ± 12	110 ± 22 (1)	nd

[a] Values in parentheses are the fold activation by putrescine. [b] Errors are standard errors of the fit. IC_{50} values were determined from the averages of the IC_{50} values (CGP 40215) at 3 different substrate concentrations (10, 32, and 80 μM) based on the relationship that $K_I = IC_{50}$, for noncompetitive inhibition (see Experimental Procedures). nd = not determined. [c] Data fitted to the Morrison equation for tight binding inhibitors gave $K_i^{app} = 0.24 \pm 0.13$ μM.

4). The addition of 5 mM putrescine abrogated the activation effect, and noncompetitive inhibition was again observed. The IC_{50} in the presence of putrescine was calculated to be 6 ± 1 μM, which is considerably lower than the value estimated in the absence of the activator. To demonstrate that the unusual kinetic behavior of CGP 48664A did not result from a contaminating molecule, the compound was purified by reversed-phase ion-pairing column chromatography (Experimental Procedures). A single peak of the correct mass eluted from the column, and the purified compound gave kinetic results identical to those of the original material.

The Effect of Mutations in the Putrescine-Binding Site of T. cruzi AdoMetDC. The putrescine-binding site in human AdoMetDC is located in the β-sheet core in a highly negatively charged region ~15 Å from the active site (Figure 1). In contrast, in the plant enzyme a series of amino acid substitutions have eliminated the site, and changed the electrostatic properties in a way that may mimic putrescine binding. The location of this site in the *T. cruzi* enzyme has not been structurally demonstrated. Our previous mutagenic data supports the idea that part, but not all, of this site is overlapping with that observed in the human enzymes; D174 appears to be important for putrescine binding in both enzymes, while the residues at positions 80, 178, and 256 are required for putrescine stimulation of the human enzyme but not the *T. cruzi* enzyme (*26*). The roles of other residues in this site have not been explored in the *T. cruzi* enzyme. The finding that putrescine can affect the catalytic properties of the enzyme, as well as modulate the mode and type of inhibition at the active site, suggests a mechanism of allosteric regulation. Energetic coupling between residues in the putrescine-binding site and the active site might be observed in this type of mechanism. In order to obtain a more detailed understanding of this mechanism we generated a series of mutant enzymes that included mutations both in the predicted putrescine-binding site (based on alignment with the human structure) and in the active site (below).

Three mutations in the predicted putrescine-binding site of the *T. cruzi* enzyme were engineered to make the sequence more like that found in the constitutively active plant enzymes: these include S111R, D174V, and F285H. The substrate kinetic profile of the D174V mutation had been previously characterized (*26*); however, inhibitor analysis had not been done. All three enzymes showed catalytic efficiency similar to that of wild-type in the absence of putrescine (Table 1). Thus, none of these mutations produced a constitutively active enzyme. The K_{act} values for putrescine were determined for each of the enzymes using a matrix of k_{cat}/K_m data collected at various putrescine concentrations. D174V was not activated by putrescine, in keeping with our previous data that putrescine no longer binds this enzyme (*26*). For S111R and F285H the K_{act} values for putrescine were 7.9 and 0.31 mM, respectively. The catalytic efficiency of S111R increases only marginally in the presence of 5 or 30 mM putrescine, thus this mutant has also lost the ability to be activated by putrescine. In contrast, although F285H exhibited a wild-type K_{act} for putrescine, its activity is stimulated to a much greater extent than that of the wild-type enzyme (360-fold compared to 27-fold, respectively), thus the fully activated enzyme has a k_{cat}/K_m that is 7-fold higher than the wild-type enzyme.

Mutations that disrupt the ability of the enzyme to bind putrescine also affected the response of the enzyme to bind inhibitors, demonstrating that these enzymes cannot be fully activated for substrate catalysis or inhibitor binding. For F285H, which still binds putrescine, the kinetics of inhibition by CGP 40215 were similar to those of wild-type. In contrast, for D174V, while the IC_{50} is similar to wild-type in the absence of putrescine, the binding is no longer sensitive to the addition of putrescine. For S111R the IC_{50} has increased by 3-fold, and it is no longer sensitive to putrescine (Table 1).

The Effect of Active Site Mutations on Putrescine Activation and Inhibitor Binding. The substrate-binding site is composed primarily of hydrophobic amino acids (Figure 1). The amidine groups of CGP 48664A form hydrogen bonds with Glu247, and the aromatic ring is sandwiched between Phe7 and Phe223. In order to determine which residues in the substrate-binding pocket may be involved in the mechanism of putrescine activation, site-directed mutagenesis was performed on residues in the pocket. Most of these residues are conserved between the human and *T. cruzi* AdoMetDC (Figure 1), and these residues were mutated to Ala in the *T. cruzi* enzyme (F7A, V64A, T245A, E247A; numbered according to the human sequence). However, four residues within 7 Å of ligand are variable between the *T. cruzi* and human enzyme. To address the possibility that these changes account for the species selective binding properties of the guanylhyrazones, these residues were mutated to their human counterpart (A5H, V52I, L221T, and C250F). Altogether

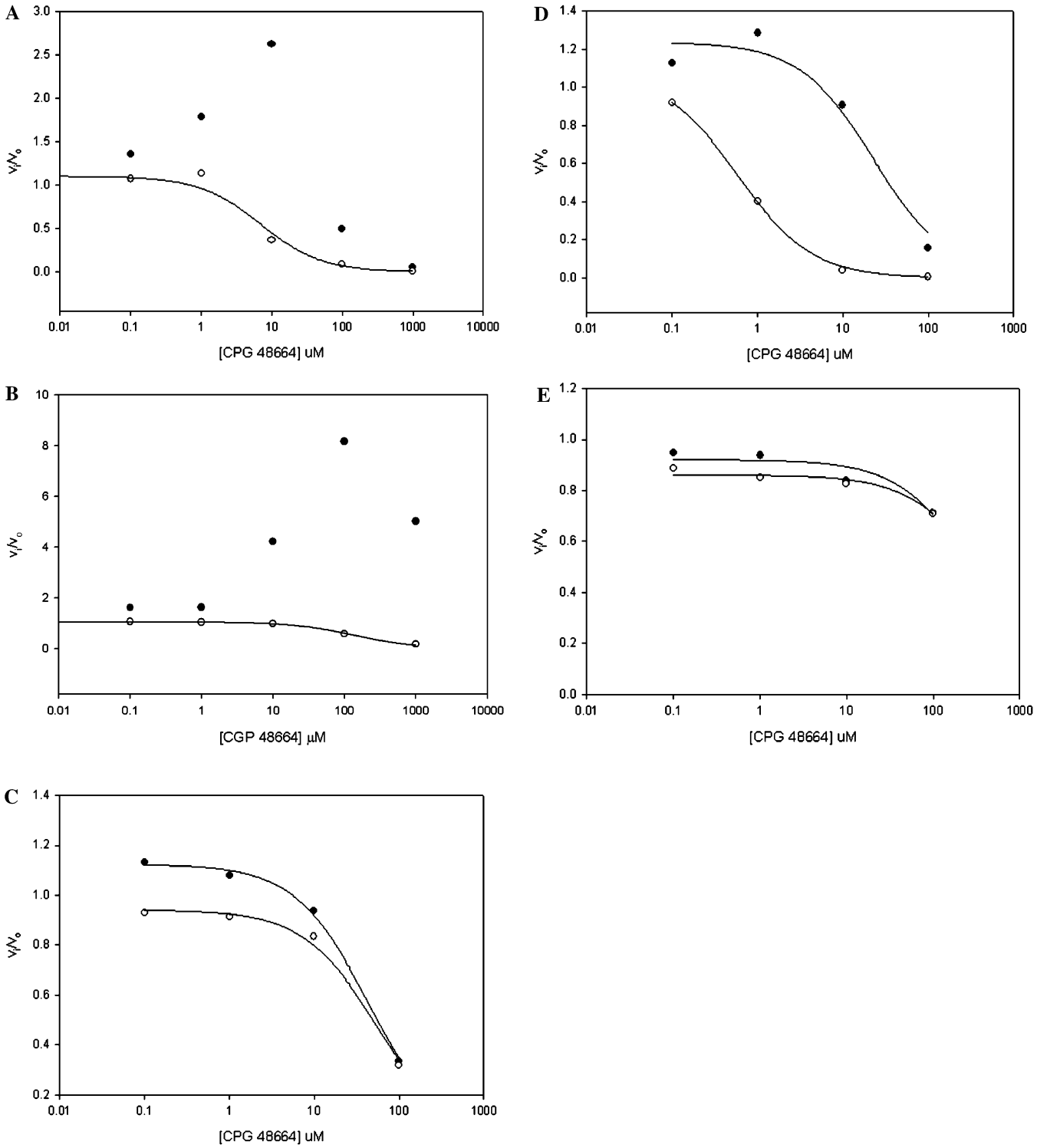

FIGURE 4: Inhibition of *T. cruzi* AdoMetDC by CGP 48664A: (A) wild-type, (B) E247A, (C) D174V, (D) L221T, and (E) D174V/E247A in the presence (open circles) and absence (filled circles) of 5 mM putrescine. Data were collected at 80 μM AdoMet.

eight mutant enzymes in the binding pocket were generated. In addition we attempted to produce F223A; however, we were unable to express this mutant protein.

Steady-state kinetic analysis of the mutant enzymes demonstrated that the A5H and V52I mutant enzymes had wild-type catalytic properties and they were activated by putrescine with a similar dose response curve (Table 2). In addition, binding of CGP 40215 was not significantly affected. The remaining mutations reduced the catalytic efficiency (k_{cat}/K_m) by 10−200-fold. While the K_{act} values for putrescine binding were similar to that of wild-type, two mutant enzymes (F7A and T245A) are impaired in their ability to respond to putrescine, and the activity was only stimulated 4-fold by the addition of activator. Thus these mutations have affected the allosteric communication between the putrescine site and the active site.

Inhibitor studies were undertaken with CGP 40215 and CGP 48664A. In addition to the large reduction in catalytic efficiency, the E247A mutation also had the largest negative impact on binding of CGP 40215; the IC_{50} was increased

by 30- and by 130-fold in the presence or absence of putrescine, respectively. The V64A and T245A mutations also increased the IC_{50} for inhibitor binding by 5−10-fold. Notably the F7A mutation did not have a large effect on binding of this inhibitor. In contrast, mutation of this residue in the human enzyme decreased binding of CGP 48664A by 1000-fold (*14*). Finally the L221T mutation, which replaces one of the species-variable residues in the pocket with the human counterpart, increased the affinity of the enzyme for CGP 40215. The IC_{50} is 3-fold lower in the absence of putrescine, and 8-fold lower than that of wild-type in the presence of putrescine. While the IC_{50} (0.4 μM) for *T. cruzi* L221T is still ~100-fold higher than observed for the human enzyme, this amino acid substitution, in part, explains the species differences in the potency of binding of CGP 40215.

Kinetic analysis of CGP 48664A is complicated by the fact that, at lower levels of inhibitor, activation of the wild-type enzyme is observed (Figure 4A). To address the structural basis for this activation we extended the analysis of this inhibitor to the two mutant enzymes that had the most profound effects either on the binding of CGP 40215 (E247A and L221T) or on putrescine activation and binding (D174V). We also generated the double mutant (E274A/D174V), which has both impaired putrescine activation and enzyme activity (Table 2). For the E274A mutant enzyme, the enzyme activation at low concentrations of inhibitor (<100 μM) was more pronounced than for the wild-type enzyme (8-fold vs 2.5-fold at the peak of activation; Figure 4). Again activation was only observed in the absence of putrescine. In the presence of putrescine, the dose response curve shows straightforward inhibition of enzyme activity ($IC_{50} = 140$ μM). For the D174V mutation, which is unable to bind putrescine, CGP 48664A displayed a simple inhibitory dose response curve ($IC_{50} = 42$ μM), and no activation was observed at any concentration of the inhibitor (Figure 4). L221T binds inhibitor with 8-fold higher affinity ($IC_{50} = 0.4$ μM) than wild-type in the presence of putrescine, and while activation was observed in the absence of putrescine, it was more modest than for the wild-type enzyme. Finally, the double mutant (E274A/D174V) was neither activated nor strongly inhibited ($IC_{50} > 300$ μM) with or without putrescine.

DISCUSSION

In mammalian cells polyamines are tightly regulated, and both ODC and AdoMetDC levels are controlled by regulation of transcription, translation, and protein stability (*3*; *36*; *2*, *37*−*39*). Like mammalian cells, yeast regulates the levels of ODC using a polyamine-sensitive degradation system (*40*), and plants control translation of AdoMetDC with a small upstream open reading frame (*41*, *42*). However, no evidence for transcriptional or translational control of polyamine levels in the trypanosomatids has been found. Some evidence for protein degradation as a mechanism of regulation has been found in *Crithidia* (*43*); however, *T. brucei* ODC is stable and is not recognized by the proteosome (*44*−*47*). Thus a key question remains: How do trypanosomes control metabolic flux through the polyamine pathway?

The mechanisms by which putrescine regulates AdoMetDC function are species specific. The specific activity of the *T. cruzi* enzyme is strongly stimulated by putrescine, which at saturating levels increases k_{cat} by 27-fold. The enzymes from the worms *Onchocerca volvulus* and *Caenorhabditis elegans* have also been reported to be strongly activated by putrescine by 60- and 350-fold, respectively (*30*, *31*), suggesting that these species also regulate polyamines in this manner. In addition, binding of active site inhibitors to the *T. cruzi* enzyme is stimulated by putrescine, resulting in a decrease in the IC_{50} of up to 10-fold. The K_{act} for putrescine binding is 0.4 mM, which is very similar to the reported levels of putrescine in trypanosome parasites (ranging from 0.1 to 0.6 mM (*10*), assuming a cell volume of 54 μM^3 (*48*)) Thus this regulation is very likely to be physiologically relevant to the function of the enzyme in the cell, and points to a mechanism by which polyamine levels are controlled in these parasites. The requirement for putrescine to stimulate the enzyme activity would protect the cell from converting AdoMet to dcAdoMet unless putrescine is present as a substrate for the formation of spermidine. Studies of α-difluoromethylornithine resistant clinical isolates of *T. brucei* have suggested an association between changes in AdoMet levels and drug toxicity (*6*). Further, since even the fully stimulated *T. cruzi* enzyme has low activity compared to the human and plant enzymes, AdoMetDC may be a central regulatory point in controlling polyamine flux in the parasite. The F285H mutant of *T. cruzi* AdoMetDC is more responsive to putrescine than the wild-type enzyme, and it has a fully stimulated activity that is 7-fold higher than the wild-type enzyme. Thus the *T. cruzi* AdoMetDC has not evolved for maximal enzyme efficiency, suggesting further that a low activity enzyme is beneficial to the parasite.

The different effects that putrescine exerts on the function of AdoMetDC from various species suggest that each enzyme has unique structural features. The putrescine-binding site in the human enzyme is distant from the active site and is located in the core of the β-sheet (Figure 1). Our previous data suggested that the putrescine site in the *T. cruzi* enzyme is partially, but not entirely, overlapping with this site (*26*). In order to gain more insight into the nature of the putrescine-binding site in the *T. cruzi* enzyme, we made a set of mutations that were designed to substitute additional residues in the *T. cruzi* sequence with those found in the plant enzyme: S111R, D174V, and F285H. Both S111R and D174V had impaired putrescine binding, and both have lost the ability to be activated by the diamine. The putrescine-stimulated activity of S111R was lower than the wild-type enzyme, and while mutation of F285H did not affect the apparent putrescine binding constant, nor the basal activity, the fully stimulated enzyme has 7-fold higher activity than the wild-type enzyme. These data suggest that the putrescine-binding site is energetically coupled to the active site, providing evidence for functional long-range interactions and allosteric control of this enzyme. It is interesting to speculate about the structural basis for the observed allostery. The *T. cruzi* enzyme may exist in two conformations (active R-state and inactive T-state) that are in equilibrium with each other, or it may assume a partially active conformation that is distinct from the fully active structures observed for the plant enzyme, or for the human enzyme bound to putrescine. The S111R and F285H mutations may shift the equilibrium toward the T-state and the R-state, respectively, or they may

induce a partial conformational change that leads to changes in activity.

The active site of AdoMetDC also has structural differences that result in species-specific enzyme function. CGP 40215 and CGP 48664A are potent inhibitors of the human enzyme, yet they are considerably less active against *T. cruzi* AdoMetDC (Table 1). These inhibitors have been demonstrated to bind the active site of the human enzyme (*14*). In *T. cruzi* AdoMetDC mutation of residues V64, T245, and E247 increases the inhibitor IC_{50}, supporting the conclusion that these residues also contact the inhibitor in the parasite enzyme. The remaining mutations had little negative impact on inhibitor binding, suggesting that the inhibitor may be oriented differently in the *T. cruzi* enzyme than in the human structure. This idea is further supported by the results of the F7A mutation. This mutation in the human enzyme decreased the binding affinity of the inhibitor by 1000-fold (*14*), while it had little impact on binding to the *T. cruzi* enzyme. F7A participates in a stacking interaction with the inhibitor in the human structure. Our data suggest that it is not optimally aligned for this interaction in the *T. cruzi* enzyme.

The *T. cruzi* enzyme contains four residues in or near the inhibitor binding site that differ in sequence from the human enzyme, suggesting that these residues may be involved in the species differences in inhibitor potency. All four residues were mutated to the human counterpart (A5H, V52I, L221T, and C250F), but only the L221T mutation had a significant impact on inhibitor binding. L221T binds CGP 40215 with 8-fold better affinity than the wild-type enzyme in the presence of putrescine. While this residue is not in van der Waals contact with CGP 48664A in the structure, CGP 40215 is a larger molecule and it may potentially make direct contact with L221. This mutation may reduce a steric clash that partially accounts for why the *T. cruzi* enzyme binds the inhibitor with lower affinity than the human enzyme. Taken together it is clear that sufficient difference exists in the structure of *T. cruzi* AdoMetDC that the development of species selective inhibitors of the parasite enzyme will be feasible.

The analysis of the active site mutations also supports the finding of energetic coupling between the putrescine-binding site and the active site. Both the F7A and T245A mutations significantly reduce the basal enzyme activity, but additionally they are no longer activated by putrescine to the same extent as the wild-type enzyme. This is despite the fact that the K_{act} for putrescine is essentially unchanged from the wild-type levels. Thus these residues appear to play a role in the communication between the putrescine-binding site and the active site of the *T. cruzi* enzyme.

Unexpectedly we also observed that the diamidine inhibitor CGP 48664A both activates and inhibits *T. cruzi* AdoMetDC. Cooperativity between subunits can explain enzyme activation by inhibitors at low inhibitor concentration (e.g. the effects of PALA on aspartate transcarbamoylase (*49*)). However, while *T. cruzi* AdoMetDC is a dimer, the dissociation constant for the dimer is higher than the concentration of enzyme used in the kinetic assays (*26*), thus it is unlikely that the dimer contributes to the unusual kinetic behavior of CGP 48664A. Instead the data suggest that CGP 48664A is able to bind to both the active site and the putrescine-binding site. When bound to the putrescine site, CGP48664A acts as an agonist and stimulates the activity of the enzyme, and when bound to the active site, it behaves as an inhibitor. The data suggest that it binds with higher affinity to the putrescine-binding site than the active site, thus it stimulates activity at lower concentrations when bound to the putrescine-binding site, and it inhibits at higher concentrations once it begins to saturate the active site. Consistent with this model, the mutation that weakens interactions with the active site (E247A) causes more pronounced activation, and it takes higher concentrations of CGP 48664A before inhibition is observed, while for the mutation (L221T) that strengthens inhibitor binding to the active site, the reverse is observed. In further support, the mutation that abolishes putrescine binding (D174V) is no longer activated by inhibitor, suggesting that this mutation also perturbs CGP 48664A binding to the allosteric site. The double mutant D174V/E247A is not activated, and it is inhibited at only very high concentrations as expected for mutations that affect interactions at both sites. These data suggest that the putrescine-binding site in *T. cruzi* AdoMetDC is promiscuous. In previous studies we tested a range of amino acids, as well as 1,3-diaminopropane, cadaverine, and spermidine for their ability to activate the enzyme (*25*). Unlike for the human and yeast enzymes (*28*, *50*), both cadaverine and 1,3-diaminopropane, but not spermidine, activated the *T. cruzi* enzyme, consistent with a broader ligand specificity for the activator site of the parasite enzyme.

In the presence of putrescine, activation by CGP 48664A is no longer observed for the wild-type or mutant enzymes. Putrescine may compete with CGP 48664A and prevent its binding to this site, or activation may simply not be observed because the addition of putrescine strengthens interactions at the active site, thus under these conditions CGP 48664A may saturate the active site at concentrations below where it binds to the putrescine site. Interestingly CGP 48664A does not activate the human enzyme, and while it would be interesting to speculate that this data points to structural differences in the putrescine-binding site between the parasite and human enzyme, this result may again be a reflection of the differential binding affinity between the two sites. Because the human enzyme binds the inhibitor with so much higher affinity (in the nM range), it may be fully inhibited at concentrations below those required for binding to the putrescine site.

CONCLUSION

The studies described herein demonstrate that *T. cruzi* AdoMetDC has evolved to be poorly optimized for enzyme activity, while being strongly regulated by physiological levels of putrescine. This suggests a mechanism whereby polyamine flux is controlled by the low activity of AdoMetDC. The mutant analysis identified several residues that are likely to be involved in communicating between the two sites, and in inducing changes in the enzyme that result in activation of its catalytic function upon putrescine binding. Finally significant structural differences in both the active site and the putrescine site are present between the *T. cruzi* and human enzyme. The identification of potent and selective inhibitors that bind to the active site seems highly feasible. Additionally, the data suggest a novel mechanism for inhibiting the enzyme. Species-specific inhibitors might be designed that inhibit activity from the allosteric putrescine

site, thus providing an alternative to active site inhibitors as an approach to inhibiting the *T. cruzi* enzyme.

ACKNOWLEDGMENT

We thank Tony Pegg for helpful discussions, and we thank Tony Michael and Mike Rosen for critical reading of the manuscript.

REFERENCES

1. Pegg, A. E., and McCann, P. P. (1992) S-adenosylmethionine decarboxylase as an enzyme target for therapy, *Pharmacol. Ther. 56*, 359−377.
2. Pegg, A. E., Xiong, H., Feith, D. J., and Shantz, L. M. (1998) S-adenosylmethionine decarboxylase: structure, function and regulation by polyamines, *Biochem. Soc. Trans. 26*, 580−586.
3. Marton, L. J., and Pegg, A. E. (1995) Polyamines as targets for therapeutic intervention, *Annu. Rev. Pharmacol. Toxicol. 35*, 55−91.
4. Fries, D. S., and Fairlamb, A. H. (2003) Antiprotozoal agents, in *Burger's Medicinal Chemistry and Drug Discovery* (Abraham, D., Ed.) pp 1033−1087, John Wiley & Sons, Inc, New York.
5. Bacchi, C. J., Nathan, H. C., Yarlett, N., Goldberg, B., McCann, P. P., Bitonti, A. J., and Sjoerdsma, A. (1992) Cure of murine Trypanosoma brucei rhodesiense infections with an S-adenosylmethionine decarboxylase inhibitor, *Antimicrob. Agents Chemother. 36*, 2736−2740.
6. Bacchi, C. J., Garofalo, J., Ciminelli, M., Rattendi, D., Goldberg, B., McCann, P. P., and Yarlett, N. (1993) Resistance to DL-α-difluoromethylornithine by clinical isolates of Trypanosoma brucei rhodesiense. Role of S-adenosylmethionine, *Biochem. Pharmacol. 46*, 471−481.
7. Bitonti, A. J., Byers, T. L., Bush, T. L., Casara, P. J., Bacchi, C. J., Clarkson, A. B., Jr., McCann, P. P., and Sjoerdsma, A. (1990) Cure of *Trypanosoma brucei brucei* and *Trypanosoma brucei rhodesiense* Infections in Mice with an Irreversible Inhibitor of S-Adenosylmethionine Decarboxylase. *Antimicrob. Agents Chemother. 34*, 1485−1490.
8. Yakubu, M. A., Majumder, S., and Kierszenbaum, F. (1993) Inhibition of S-adenosyl-L-methionine (adomet) decarboxylase by the decarboxylated adomet analog 5′{[(Z)-4-amino-2-butenyl]-methylamino}-5′-deoxyadenosine (MDL73811) decreases the capacities of Trypanosoma cruzi to infect and multiply within a mammalian host cell, *J. Parasitol. 79*, 525−532.
9. Ariyanayagam, M. R., and Fairlamb, A. H. (1997) Diamine auxotrophy may be a universal feature of Tryapnsoma cruzi epimastigotes, *Mol. Biochem. Parasitol. 84*, 111−121.
10. Fairlamb, A. H., and Le Quesne, S. A. (1997) Polyamine metabolism in Trypanosomes, in *Trypanosomiasis and Leishmaniasis* (Hide, G., Mottram, J., Coombs, G., and Holmes, P., Eds.) pp 149−161, CAB International, Wallingford, Oxon, U.K.
11. Persson, K., Aslund, L., Grahn, B., Hanke, J., and Heby, O. (1998) *Trypanosoma cruzi* has not lost its S-adenosylmethionine decarboxylase: characterization of the gene and the encoded enzyme, *Biochem. J. 333*, 527−537.
12. Ekstrom, J. L., Mathews, I. I., Stanley, B. A., Pegg, A. E., and Ealick, S. E. (1999) The crystal structure of human S-adenosylmethionine decarboxylase at 2.25 Å resolution reveals a novel fold, *Structure 7*, 583−595.
13. Ekstrom, J. L., Tolbert, W. D., Xiong, H., Pegg, A. E., and Ealick, S. E. (2001) Structure of a human S-adenosylmethionine decarboxylase self-processing ester intermediate and mechanism of putrescine stimulation of processing as revealed by the H243A mutant, *Biochemistry 40*, 9495−9504.
14. Tolbert, W. D., Ekstrom, J. L., Mathews, I. I., Secrist, J. A., Kappor, P., Pegg, A. E., and Ealick, S. E. (2001) The structural basis for substrate specificity and inhibition of human S-adenosylmethionine decarboxylase, *Biochemistry 40*, 9484−9494.
15. Bennett, E. M., Ekstrom, J. L., Pegg, A. E., and Ealick, S. E. (2002) Monomeric *S*-adenosylmethionine decarboxylase from plants provides an alternative to putrescine stimulation, *Biochemistry 41*, 14509−14517.
16. Xiong, H., and Pegg, A. E. (1999) Mechanistic studies of the processing of human S-adenosylmethionine decarboxylase proenzyme, *J. Biol. Chem. 274*, 35059−35066.
17. Xiong, H., Stanley, B. A., Tekwani, B. L., and Pegg, A. E. (1997) Processing of mammalian and plant S-adenosylmethionine decarboxylase proenzymes, *J. Biol. Chem. 272*, 28342−28348.
18. Xiong, H., Stanley, B. A., and Pegg, A. E. (1999) Role of Cysteine-82 in the catalytic mechanism of human S-adenosylmethionine decarboxylase, *Biochemistry 38*, 2462−2470.
19. Stanley, B. A., Pegg, A. E., and Holm, I. (1989) Site of Pyruvate Formation and Processing of Mammalian S-Adenosylmethionine Decarboxylase Proenzyme, *J. Biol. Chem. 264*, 21073−21079.
20. Stanley, B. A., and Pegg, A. E. (1991) Amino acid residues necessary for putrescine stimulation of human S-adenosylmethionine decarboxylase proenzyme processing and catalytic activity, *J. Biol. Chem. 266*, 18502−18506.
21. Kinch, L. N., and Phillips, M. A. (2000) Single turnover analysis of *Trypanosoma cruzi* S-adenosylmethionine decarboxylase, *Biochemistry 39*, 3336−3343.
22. Park, S. J., and Cho, Y. D. (1999) Identification of functionally important residues of Arabidopsis thaliana S-adenosylmethionine decarboxylase, *J. Biochem. (Tokyo) 126*, 996−1003.
23. Schroder, G., and Schroder, J. (1995) cDNAs for S-adenosyl-L-methionine decarboxylase from Catharanthus roseus, heterologous expression, identification of the proenzyme-processing site, evidence for the presence of both subunits in the active enzyme, and a conserved region in the 5′ mRNA leader, *Eur. J. Biochem. 228*, 74−78.
24. Choi, Y. S., and Cho, Y. D. (1994) A new S-adenosylmethionine decarboxylase from soybean axes, *Biochim. Biophys. Acta 1201*, 466−472.
25. Kinch, L. N., Scott, J., Ullman, B., and Phillips, M. A. (1999) S-adenosylmethionine from *Trypanosoma cruzi*: cloning, expression and kinetic characterization of the recombinant enzyme, *Mol. Biochem. Parasitol. 101*, 1−11.
26. Clyne, T., Kinch, L. N., and Phillips, M. A. (2002) Putrescine activation of *Trypanosoma cruzi* S-adenosylmethionine decarboxylase, *Biochemistry 41*, 13207−13261.
27. Tekwani, B. L., Bacchi, C. J., and Pegg, A. E. (1992) Putrescine activated S-adenosylmethionine decarboxylase from Trypanosoma brucei brucei, *Mol. Cell. Biochem. 117*, 53−61.
28. Poso, H., Hannonen, P., Himberg, J., and Janne, J. (1976) Adenosylmethionine decarboxylase from various organisms: relation of the putrescine activation of the enzyme to the ability of the organism to synthesize spermine, *Biochem. Biophys. Res. Commun. 68*, 227−234.
29. Hoyt, M. A., Williams-Abbott, L. J., Pitkin, J. W., and Davis, R. H. (2000) Cloning and expression of the S-adenosylmethionine decarboyxlase gene of Neurospora crassa and processing of its product, *Mol. Gen. Genet. 263*, 664−673.
30. Ndjonka, D., Da'dara, A. A., Walter, R. D., and Luersen, K. (2003) Caenorhabditis elegans S-adenosylmethionine decarboxylase is highly stimulated by putrescine but exhibits a low specificity for activator binding, *Biol. Chem. 384*, 83−91.
31. Ndjonka, D., Zou, Y., Bi, X., Woster, P., Walter, R. D., and Luersen, K. (2003) The activator-binding site of Onchocerca volvulus S-adenosylmethionine decarboxylase, a potential drug target, *Biol. Chem. 384*, 1195−1201.
32. Stanley, B. A., Shantz, L. M., and Pegg, A. E. (1994) Expression of mammalian *S*-adenosylmethionine decarboxylase in *Escherichia coli*, *J. Biol. Chem. 269*, 7901−7907.
33. Osterman, A. L., Brooks, H. B., Jackson, L., Abbott, J. J., and Phillips, M. A. (1999) Lys-69 plays a key role in catalysis by *T. brucei* ornithine decarboxylase through acceleration of the substrate binding, decarboxylation and product release steps, *Biochemistry 38*, 11814−11826.
34. Williams, J. W., and Morrison, J. F. (1979) *Methods Enzymol. 63*, 437.
35. Kern, W., Schleyer, E., Bergmann, M., Gschaidmeier, H., Ehninger, G., Hiddemann, W., and Braess, J. (2001) Detection and separation of the S-adenosylmethionine-decarboxylase inhibitor SAM486A in human plasma and urine by reversed-phase ion-pairing high-performance liquid chromatography, *J. Pharmacol. Toxicol. Methods 45*, 175−180.
36. Coffino, P. (2001) Regulation of cellular polyamines by antizyme, *Nat. Rev. Mol. Cell Biol. 2*, 188−194.
37. Ivanov, I. P, Matsufuji, S., Murakami, Y., Gesteland, R. F., and Atkins, J. F. (2000) Conservation of polyamine regulation by translational frameshifting from yeast to mammals, *EMBO J. 19*, 1907−1917.
38. Morgan, D. M. L. (1999) Polyamines: an overview, *Mol. Biotechnol. 11*, 229−250.

39. Shantz, L. M., and Pegg, A. E. (1999) Translational regulation of ornithine decarboxylase and other enzymes of the polyamine pathway, *Int. J. Biochem. Cell Biol. 31*, 107−122.
40. Toth, C., and Coffino, P. (1999) Regulated degradation of yeast ornithine decarboxylase, *J. Biol. Chem. 274*, 25921−25926.
41. Hanfrey, C., Franceschetti, M., Mayer, M. J., Illingworth, C., and Michael, A. J. (2002) Abrogation of upstream open reading frame-mediated translational control of a plant S-adenosylmethionine decarboxylase results in polyamine disruption and growth perturbations, *J. Biol. Chem. 277*, 44131−44139.
42. Hanfrey, C., Elliott, K. A., Franceschetti, M., Mayer, M. J., Illingworth, C., and Michael, A. J. (2005) A dual upstream open reading frame-based autoregulatory circuit controlling polyamine-responsive translation, *J. Biol. Chem. 280*, 39229−39237.
43. Persson, L., Jeppsson, A., and Nasizadeh, S. (2003) Turnover of trypanosomal ornithine decarboxylases, *Biochem. Soc. Trans. 31*, 411−414.
44. Ghoda, L., Phillips, M. A., Bass, K. E., Wang, C. C., and Coffino, P. (1990) Trypanosome Ornithine Decarboxylase Is Stable Because It Lacks Sequences Found in the Carboxyl Terminus of the Mouse Enzyme Which Target the Latter For Intracellular Degradation, *J. Biol. Chem. 265*, 11823−11826.
45. Hua, S., Li, X., Coffino, P., and Wang, C. C. (1995) Rat antizyme inhibits the activity but does not promote the degradation of mouse ornithine decarboxylase in Trypanosoma brucei, *J. Biol. Chem. 270*, 10264−10271.
46. Phillips, M. A., Coffino, P., and Wang, C. C. (1987) Cloning and Sequencing of the Ornithine Decarboxylase Gene from *Trypanosoma brucei*. Implications for Enzyme Turnover and Selective a-Difluoromethylornithine Inhibition, *J. Biol. Chem. 262*, 8721−8727.
47. Bass, K. E., and Wang, C. C. (1991) The in vitro differentiation of pleomorphic Trypanosoma brucei from bloodstream into procyclic form requires neither intermediary nor short-stumpy stage, *Mol. Biochem. Parasitol. 44*, 261−270.
48. Ghiotto, V., Brun, R., Jenni, L., and Hecker, H. (1979) Trypanosoma brucei: morphometric changes and loss of infectivity during transformation of bloodstream forms to procyclic culture forms in vitro, *Exp. Parasitol. 48*, 447−456.
49. Foote, J., and Schachman, H. K. (1985) Homotropic effects in aspartate transcarbamoylase. What happens when the enzyme binds a single molecule of the bisubstrate analog N-phosphonacetyl-L-aspartate? *J. Mol. Biol. 186*, 175−184.
50. Pegg, A. E., and Williams-Ashman, H. G. (1968) Stimulation of the decarboxylation of S-adenosylmethionine by putrescine in mammalian tissues, *Biochem. Biophys. Res. Commun. 30*, 76−82.

BI0603975